Environmental Pollution 360 (2024) 124642

Contents lists available at ScienceDirect

Environmental Pollution

journal homepage: www.elsevier.com/locate/envpol

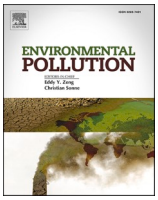

Reflections of stress: Ozone damage in broadleaf saplings can be identified from hyperspectral leaf reflectance☆

Anna Lee Jones [a,*], Adam Ormondroyd [b], Felicity Hayes [c,1], Elizabeth S. Jeffers [a,1]

[a] Department of Biology, University of Oxford, South Parks Road, Oxford, OX13SZ, UK
[b] Kavli Institute for Cosmology, University of Cambridge, Madingley Road, Cambridge, CB3 0HA, UK
[c] UK Centre for Ecology & Hydrology, Environment Centre Wales, Deiniol Road, Bangor, LL57 2UW, UK

ARTICLE INFO

Keywords:
Tropospheric ozone
Reflectance spectroscopy
Forest monitoring
Temperate forest
Air pollution
Vegetation index

ABSTRACT

Tropospheric ozone (O_3) causes widespread damage to vegetation; however, monitoring of O_3 induced damage is often reliant on manual leaf inspection. Reflectance spectroscopy of vegetation can identify and detect unique spectral signatures of different abiotic and biotic stressors. In this study, we tested the use of hyperspectral leaf reflectance to detect O_3 stress in alder, beech, birch, crab apple, and oak saplings exposed to five long-term O_3 regimes (ranging from daily target maxima of 30 ppb O_3 to 110 ppb). Hyperspectral reflectance varied significantly between O_3 treatments, both in whole spectra analysis and when simplified to representative components. O_3 damage had a multivariate impact on leaf reflectance, underpinned by changes in pigment balance, water content and structural composition. Vegetation indices derived from reflectance which characterised the visible green peak were able to differentiate between O_3 treatments. Iterative normalised difference spectral indices across the hyperspectral wavelength range were correlated to visual damage scores to identify significant wavelengths for O_3 damage detection. We propose a new Ozone Damage Index (OzDI), which characterises the reflectance peak in the shortwave infrared region and outperformed existing vegetation indices in terms of correlation to O_3 treatment. These results demonstrate the potential application of hyperspectral reflectance as a high throughput method of O_3 damage detection in a range of common broadleaf.
species.

1. Introduction

At ground level, O_3 is a highly oxidising pollutant which is toxic to both plant (Ainsworth et al., 2012) and animal life (Nuvolone et al., 2018), and is a potent greenhouse gas (Mickley et al., 1999). Tropospheric O_3 is formed by photocatalysis of a free radical mechanism between nitrous oxides (NO_x), hydrocarbons, and volatile organic compounds (VOCs) (Levy, 1971).

Tropospheric O_3 pollution has increased globally since 1950s (Vingarzan, 2004), and although O_3 precursor emissions have plateaued in Europe and North America since the 1990s resulting in a decrease in extreme O_3 events, long-range transport of anthropogenic O_3 precursors continues to raise European baselines (Gaudel et al., 2018). Background tropospheric O_3 concentrations are predicted to continue to rise in the northern hemisphere until at least the end of the century. O_3 induced injury is widespread in European vegetation, including crops (Mills et al., 2011) and trees (Gottardini et al., 2016).

O_3 uptake causes oxidative damage to plants by the oxidation of lipids, peptides, and nucleic acids through the induction of reactive oxygen species (ROS) (Francini et al., 2007). ROS alter rubisco activity and content (Saxe, 2002), leading to photoinhibition. Stomatal conductance is reduced in response to O_3 which limits transpiration and CO_2 uptake (Victoria et al., 2007). O_3 can be detoxified within the plant by antioxidising compounds such as superoxide dismutase and peroxidases (Kangasjarvi et al., 1994).

Foliar O_3 damage includes stippling, chlorosis and necrosis (Sicard et al., 2010), and can be visually differentiated from other biotic and abiotic stressors in broadleaf trees by the size, shape, and location of the damage (Brace et al., 1999; Treshow, 1970). Stippling occurs on the upper leaf surface between veins as dots of brown to black pigmentation.

☆ This paper has been recommended for acceptance by Dr Alessandra De Marco.

* Corresponding author. Department of Biology, University of Oxford, South Parks Road, Oxford, OX1 3SZ, UK.
E-mail address: anna.jones@biology.ox.ac.uk (A. Lee Jones).

[1] Joint senior authors.

https://doi.org/10.1016/j.envpol.2024.124642
Received 7 June 2024; Received in revised form 26 July 2024; Accepted 29 July 2024
Available online 31 July 2024
0269-7491/© 2024 The Authors. Published by Elsevier Ltd. This is an open access article under the CC BY license (http://creativecommons.org/licenses/by/4.0/).

Chlorosis is a loss of chlorophyll and appears in discrete patches known as mottles. Small discrete areas of dead tissue in the palisade mesophyll, known as fleck, also occur.

O_3 stressed vegetation shows decreased primary productivity (Ashmore, 2005), which limits the ability of vegetation to produce biomass and sequester carbon. Models based on experimental data estimate the reduction in the gross primary productivity (GPP) of European forests due to O_3 stress from 2000 to 2010 range between 0.4% and 30% (Proietti et al., 2016). Verification of the extent and location of O_3 damage to forest landscapes would be required to confirm the reduction of GPP attributable to O_3 exposure. Furthermore, the impact of long-term or variable O_3 exposure on ecosystem productivity is complex to predict due to the interacting effects of O_3 stress with temperature, carbon dioxide (CO_2), water, and nitrogen availability.

Visible foliar O_3 injury is variable between species and requires experienced human identification to differentiate it from other stressors, and crown defoliation is not specific to O_3 stress (Brace et al., 1999). Full assessment of foliar O_3 damage also requires access to the upper crown exposed to the sun (Schaub et al., 2016). A versatile and efficient method of measuring O_3 damage to trees would allow more widespread monitoring of the impacts of O_3 and justify responses in terms of precursor emissions control and species selection for O_3 exposed

sites.

Vegetation spectroscopy uses the light reflectance or fluorescence of living vegetation to assess plant health at a variety of spatial scales. The high-throughput nature of spectroscopy allows rapid and non-destructive monitoring of plant health, including remote monitoring of large or inaccessible areas when spectroscopic instruments are mounted on unmanned aerial vehicles, aircraft, or satellites. Field spectroscopy, taken at the single plant or leaf level provides a higher signal-to-noise ratio measurement than remote spectroscopy but is still comparable to satellite-derived spectral signatures, and can be correlated to physiological and biochemical measurements taken in situ. Field spectroscopy, therefore, bridges the spatial gap between leaf-level measurements of productivity and ecosystem measurements of plant health derived from satellite data.

Symptoms of acute O_3 exposure such as visible foliar injury have been successfully detected using vegetation indices in some O_3 sensitive species (Diem, 2002; Kefauver, 2013). Reflectance spectroscopy has detected O_3 stress in leaves before injury is visible for several sensitive species such as white clover (Meroni et al., 2008a), soybean (Gosselin et al., 2020; Moon et al., 2004), pomegranate (Calzone et al., 2021), and sage (Marchica and Cotrozzi, 2019). Similar techniques have been applied to a few tree species, such as the study by Gäb et al. on *Fagus sylvatica* (common beech), which used near-infrared (NIR) spectroscopy to successfully predict the concentration of O_3 treatment during one growth season (Gab et al., 2006).

Spectroscopic detection of O_3 damage has not been trialled in temperate broadleaf tree species beyond common beech. Most trials have also focused on acute O_3 exposure in the range of 200 ppb for relatively short periods (24h to one month) (Meroni et al., 2008b; Marchica and Cotrozzi, 2019; Calzone et al., 2021). Chronic O_3 exposure (such as 60 ppb during daylight hours for several weeks) is more commonly experienced by broadleaf forests and is predicted to increase over the next century (Intergovernmental Panel on Climate Change (IPCC), 2023). Considering this, detecting damage to vegetation exposed realistic long-term O_3 concentrations is most relevant to the management of terrestrial carbon stocks.

This study aimed to characterise the reflectance profile of O_3 damage in a range of temperate broadleaf species under controlled conditions. We set out to test whether hyperspectral reflectance measurements could differentiate between saplings exposed to different O_3 regimes. Based on the successful detection of acute O_3 damage by reflectance spectroscopy in sensitive crops, we predicted clear differences in the spectral signatures of saplings exposed to ambient versus elevated O_3. The high resolution of hyperspectral leaf reflectance also has the potential to differentiate more finely between intermediate O_3 concentrations. Different tree species show varying degrees of O_3 sensitivity (Hayes et al., 2015) and so we also expected species specific responses to be visible in the reflectance signature of O_3 stress. We chose a mixture of temperate species common to broadleaf forests, reforestation, and hedge planting initiatives, which are reported to have varying tolerance to O_3 (Feng, 2018). A nitrogenfixing species, alder, was included based on evidence that nitrogen-fixing symbioses offer some resistance to O_3 stress (Hayes et al., 2015). In the context of reforestation initiatives, O_3 damage detection in cell grown saplings is particularly pertinent.

2. Material and methods

2.1. Plant materials

On April 4, 2022, twenty cell-grown, two-year-old alder (*Alnus cordata*), birch (*Betula pendula*), crab apple (*Malus sylvestris*), oak (*Quercus robur)*, beech (*Fagus sylvatica*) saplings (Cheviot Trees Ltd, UK) were potted into 6.5L tubs containing a 3:1 ratio by volume of peat-free Nursery Stock compost (Sinclair, UK) and John Innes No.2 (J. Arthur Bowers, UK). Saplings were kept outside for 4 weeks at the Air Pollution Facility to establish before O_3 treatment began. Saplings were irrigated by hand three times weekly with additional watering on days of hot weather. On June 2, 2022, the saplings were stratified into three height categories by species. From these groups, the saplings were randomly distributed between five O_3 treatments at ambient temperature. The saplings were exposed to experimental conditions in the solardomes from June 2, 2022 until October 14, 2022.

2.2. Treatments

This experiment took place at the UK Center for Ecology & Hydrology's air pollution facility at Abergwyngregyn, North Wales (53.2°N, 4.0°W). O_3 was delivered in solardomes, dome-shaped glasshouses of 3m diameter and 2.1m height as described previously (Hayes et al., 2015).

The solardomes were ventilated at two air changes per minute with charcoal filtered air to which O_3 was added to give the desired concentration. O_3 was generated using concentrated oxygen (PT20 O_3 generator, Ozone Industries, and AirSep NewLife Intensity 10L Oxygen Concentrator, CAIRE Inc. USA). O_3 delivery was controlled by LabVIEW software (version 2015, National Instruments, USA). O_3 concentrations within the solardomes were measured every 30min (for 5min) using two O_3 analysers (49i Thermo Fisher Scientific, USA) of matched calibration. Air temperature, relative humidity, and light were also monitored inside the solardomes (Skye Instruments, UK).

The solardomes' weekly O_3 profiles were based on data from a UK upland O_3 episode as previously described (Hayes et al., 2015), and target concentrations were increases above and below this profile. The weekly O_3 profile featured five consecutive "high" O_3 days where the O_3 concentration was raised from 20 ppb overnight to the target maximum from 10:00–18:00, followed by two "low" O_3 days where concentration for all domes peaked at 30 ppb. This profile better replicates the dynamics of real O_3 episodes than a constant elevated exposure regime and has been used for many successful O_3 exposure experiments (Brewster et al., 2024; Hattie et al., 2022; Amanda et al., 2022). The target peaks of the five solardomes were 30 ppb, 50 ppb, 65 ppb, 80 ppb, and 110 ppb. The seasonal averages of the O_3 concentration per treatment dome are summarised in Table 1.

2.3. Plant measurements

2.3.1. Growth

After one month of O_3 treatment and again after four months, the height and diameter of the basal stem were measured for all saplings. The relative difference in height and basal stem diameter between

Table 1
Average O_3 concentrations, test species and number of replicates per solardome. Daytime is defined as 10:00–18:00.

O_3 Treatment	Seasonal O_3 24h average (ppb)	Daytime O_3 average (ppb)	Daytime Average AOT40 (ppb)	Sapling species	Number of replicates per species
OZ1, lowest O_3	23.29	25.76	0	Oak, beech, crab apple, alder, birch	3, 3, 5, 5, 5 (respectively)
OZ2, low O_3	32.97	39.16	5.37	Oak, beech, crab apple, alder, birch	3, 3, 5, 5, 5 (respectively)
OZ3, medium O_3	36.65	47.97	12.11	Oak, beech, crab apple, alder, birch	3, 3, 5, 5, 5 (respectively)
OZ4, high O_3	38.16	56.31	21.68	Oak, beech, crab apple, alder, birch	3, 3, 5, 5, 5 (respectively)
OZ5, highest O_3	45.87	66.63	31.53	Oak, beech, crab apple, alder, birch	3, 3, 5, 5, 5 (respectively)

months one and four was calculated as a percentage growth over the treatment period. Alder, birch, and crab apple saplings were measured again in August 2023 after wintering outside under ambient conditions.

2.3.2. O_3 damage score

The extent of visible foliar O_3 damage to saplings each month was determined according to the following simple damage score devised to be time efficient and applicable to all test species. Damage score 1, healthy green leaves with no visible O_3 damage. Damage score 2, interveinal stippling or mottles on less than half of the leaves, by area or percentage of affected leaves. Damage score 3, stippling or mottles on half or more of the leaves, by area or percentage of affected leaves. Damage score 4, stippling or mottles present and flecks covering less than half the leaves, by area or percentage of leaves affected. Damage score 5, stippling or mottles present and flecks of over half the leaves, by area or percentage of leaves affected. Images exemplifying each damage score are included in the supplementary material. Mean damage score for each species and treatment per month was calculated.

Any other notable observations about sapling health were also recorded monthly.

2.4. Leaf spectroscopy

Reflectance spectra of the adaxial leaf surface from 350 nm to 2500 nm were collected using an HR-1024i with leaf clip, Spectra Vista Corp, USA including an active light source. The HR-1024i spectrometer consisted of three dispersion grating spectrometers with overlapping wavelength ranges:

VNIR, 1.5 nm sampling interval, 350 nm–1000 nm range; SWIR1, 3.8 nm sampling interval, 1000 nm–1890 nm range; SWIR2, 2.5 nm sampling interval, 1890 nm–2500 nm range.

The spectrometer was referenced using the incorporated leaf clip reflective standard every 5 min during measurements. Dark signal baseline correction was applied by the HR-1024i automatically, a dark spectrum was taken before each reflectance measurement. Once per month during O_3 treatment, reflectance spectra were taken from three leaves from three replicates of each species per O_3 treatment. The three leaves were chosen as one from each third of the vertical span of the sapling's leaf cover.

2.4.1. Spectral analysis

Reflectance spectra were imported and processed as a spectral library in Python 3 using the SpecDAL package (Lee; Van Rossum and Drake, 2009). The overlapping regions of the three component spectrometers in the HR-1024i were stitched. Reflectance measurements were interpolated to correspond to 1.0 nm interval wavelengths. The absolute reflectance was derived by multiplying the relative reflectance by the known reflectance of the reference panel.

Further processing of the spectral library was carried out in R using the hyperSpec package (Beleites and Sergo). An average reflectance spectrum was calculated for each species, month and O_3 treatment.

Permutational multivariate analysis of variance (PERMANOVA) was performed using the vegan R package (Oksanen et al., 2008) as a non-parametric geometric partitioning of variance to test the contributions of species, O_3 treatment and length of exposure as explanatory factors of spectral variation. The Bray method was used to calculate pairwise distances from the spectral matrix and 999 permutations were used.

Principal component analysis (PCA) was used to visualise the key regions of variability within the hyperspectral library by dimensionality reduction. PCA was applied to the entire range of wavelengths measured 350 nm to 2500 nm. Principle components of the spectral library were calculated for each O_3 treatment and species.

Partial least squares discriminant analysis (PLS-DA) was used as an extension of PCA to build classification models based on principal components. We built a PLS-DA model which predicted the O_3 treatment leaves had been exposed to based on their hyperspectral reflectance spectra (350 nm–2500 nm). PLS-DA was used due to the ordinal nature of the O_3 treatments in this experiment. PLS-DA was used built using the mdatools R package (Kucheryavskiy, 2020). For each species, the optimum number of principle components was assessed to maximise the model's accuracy. A randomly selected 70% of the spectral library was used to calibrate the model and the remaining 30% used to cross validate it.

2.4.2. Vegetation indices

A range of vegetation indices which correlate to plant health and stress were calculated from leaf reflectance data and assessed for their ability to distinguish between O_3 treatments. Full equations for all vegetation indices calculated can be found in the supplementary material (Table A.3).

2.4.3. Normalised difference spectral indices

To identify the spectral wavelengths that could best indicate O_3 damage, normalised difference spectral indices (NDSI) analysis was used. NDSI is defined as:

$$NDSI(i,j) = \frac{R_i - R_j}{R_i + R_j} \quad (1)$$

where R_i is the absolute reflectance of wavelength i and subscripts are wavelengths in nm. All possible combinations of wavelengths (i and j) were used to calculate all NDSI for each plant species, month and treatment. The linear relationships between the average O_3 damage score and NDSIs per species, month and treatment were examined. A heat map of the absolute value of the Pearson correlation coefficient r between O_3 damage score and NDSI was generated using data collected throughout the growing season. The heat maps were produced using

Python 3 packages: correlation arrays were created using NumPy, and plotted with matplotlib (Charles et al., 2020; Hunter, 2007).

2.5. Statistical analysis

Statistical analysis of the results of sapling growth and vegetation indices derived from reflectance data, were carried out in R using the inbuilt Stats package and mdatools. Non-parametric tests were used where data failed to pass normality and homogeneity of variance testing, as detailed in results.

3. Results

3.1. Plant measurements

3.1.1. Growth

O_3 treatment did not significantly affect the percentage growth of saplings between June and October 2022, as tested with the Kruskal-Wallis chi-square test ($\chi^2 = 9.5791$, d.o.f. $= 6$, $P = 0.144$). The interaction between species and O_3 treatment was also not significant ($F = 3.2419$, d.o.f. $= 22$, $P = 0.344$).

Alder, birch, and crab apple saplings were overwintered in ambient conditions (October 2022–May 2023) and then returned to their previous ozone treatment domes for a further growth season. O_3 treatment had a significant effect on change in height between October 2022 and August 2023 (ANOVA, $F(2,42) = 5.21$, $P < 0.01$) (supplementary material Figure A.8). Post hoc analysis using the Tukey HSD test indicates that saplings exposed to high O_3 treatment (OZ5) grew significantly less between October 2022 and August 2023 (mean = 1.47, std. dev. = 5.41) than saplings in either the intermediate (mean = 8.56, std. dev. = 7.59) or low (mean = 8.31, std. dev. = 7.28) $O_{3\text{treatments}}$.

3.1.2. O_3 damage score

The O_3 induced damage scores of saplings increased with elevated O_3 treatment (Fig. 1). Ordinal logistic regression between average O_3 damage score and O_3 treatment showed that for each unit increase in average damage score, the odds ratio of the sapling being exposed to high O_3 treatment increased on average by 12.94 ($P = 8.34 \times 10^{-5}$). Furthermore, McFadden's pseudo-R^2 value for this model was estimated to be 0.403, thereby indicating a robust positive correlation between O_3 damage score and the concentration of O_3 treatment.

When separated by species, all species except crab apple show increasing O_3 damage scores under higher O_3 treatments. Crab apple saplings showed a more mixed pattern, although damage free saplings (score 1) were only found in the lower O_3 treatments.

3.2. Leaf spectroscopy

3.2.1. Leaf clip reflectance

For each species, leaf clip reflectance spectroscopy showed clear differences between the spectra of saplings grown in different O_3 treatments (Fig. 2).

Key regions of differentiation between O_3 treatments included the green peak in the visible range (~540 nm); the NIR region (800 nm–1500 nm); the water absorption bands at 1440 nm and 1900 nm; and the infrared peak at 2220 nm. In July in the highest O_3 treatment, reflectance spectra feature an absorption peak at 750 nm caused by chlorophyll fluorescence.

In the visible light region of the spectra, the trough in reflectance between 400 nm–500 nm caused by absorbance of blue/violet light by chlorophyll A is shallower in saplings exposed to high O_3 concentrations. When all species are averaged, the reflectance trough is deepest in saplings exposed to ambient O_3 (OZ1) and shallowest in saplings exposed to the highest O_3 treatment (OZ5), indicating lower chlorophyll.

The green reflectance peak at 550 nm attributed to chlorophyll, and is reduced in saplings exposed to the highest O_3 concentration (OZ5) compared to ambient conditions (OZ1) when all species are averaged. At the species level, beech, birch, and crab apple saplings all show a reduced green peak when exposed to high O_3 concentration. However,

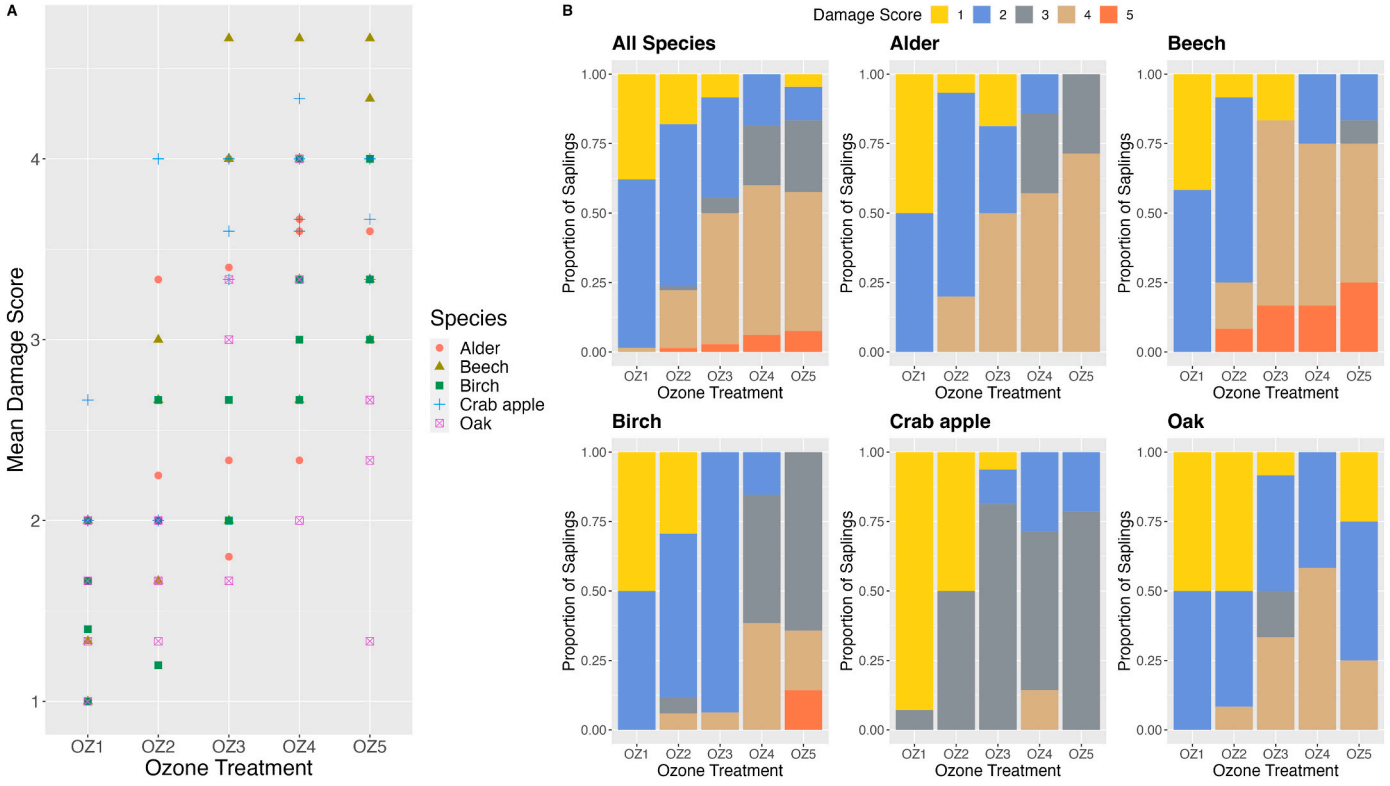

Fig. 1. O_3 damage to saplings following exposure to O_3 with A) Mean O_3 damage score and B) proportion of saplings in each damage category.

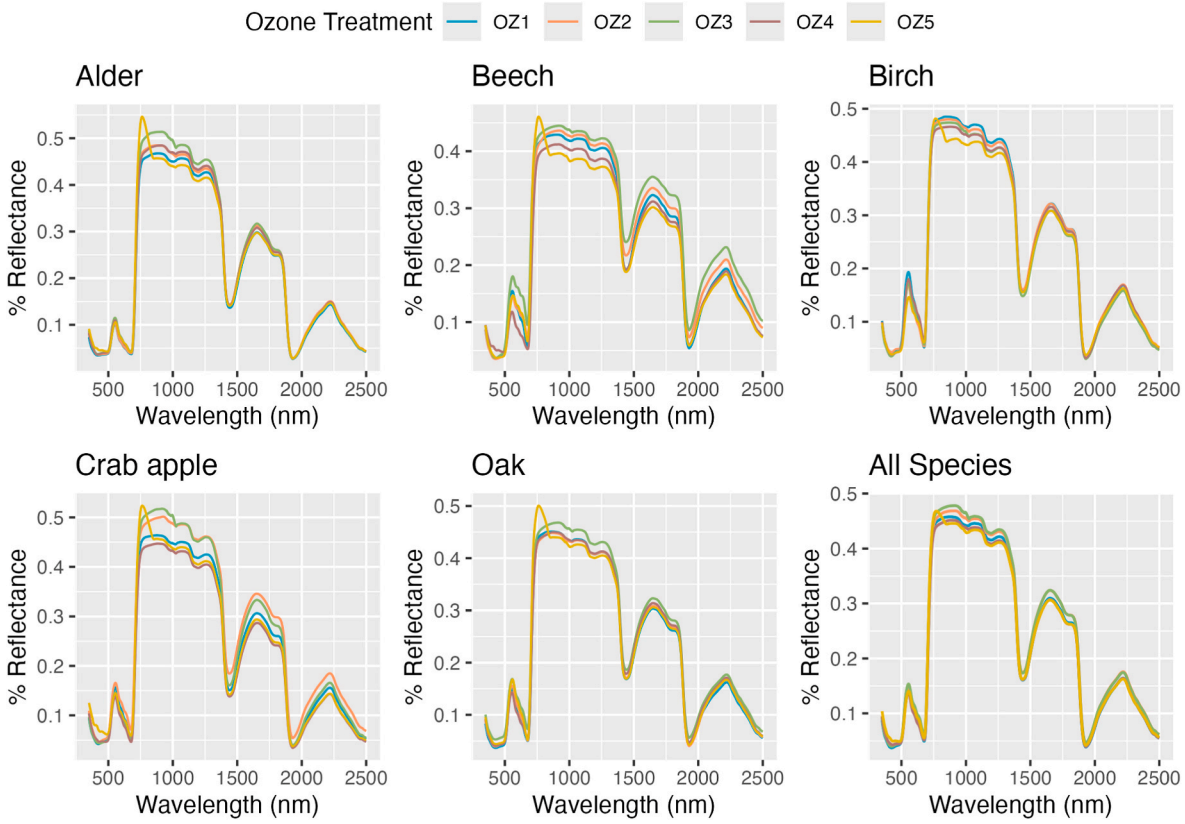

Fig. 2. Monthly average leaf clip reflectance spectra from alder, beech, birch, crab apple, oak saplings exposed to different O_3 treatments, July to October 2022.

alder and oak saplings had increased green peak reflectance under high O_3 conditions.

The reflective region in the NIR characterised by three broad peaks between 750 nm and 1400 nm is attributed to cell structure. High O_3 exposure reduced the NIR reflectance of saplings. This was particularly marked in alder, beech, and birch saplings. In all species except birch, saplings exposed to intermediate O_3 (OZ3) had the highest NIR reflectance.

The water absorption bands at 1440 nm and 1900 nm were slightly reduced in saplings exposed to higher O_3 concentrations. This was most marked in crab apple and beech. In all species, saplings exposed to intermediate O_3 concentration (OZ3) had increased reflectance between 1440 nm and 1900 nm.

The SWIR reflectance peak at 2220 nm is associated with cellulose, sugar, and starch content of the leaf (Curran, 1989). In beech, crab apple, and birch saplings this reflectance peak was reduced under high O_3 exposure (OZ5) compared to ambient exposure (OZ1). Conversely, in alder and oak the 2220 nm reflectance peak was slightly higher in saplings exposed to the highest O_3 concentration (OZ5) than those exposed to ambient concentration (OZ1). In all species except birch, saplings exposed to intermediate O_3 concentration (OZ3) had a higher 2220 nm reflectance peak than saplings exposed to ambient (OZ1) or high O_3 (OZ5).

Two-way permutation analysis of variance showed that the effect of species, O_3 treatment (and the interaction between the two) were significant on the reflectance spectra of sapling leaves (supplementary material Table A.5). When each month's spectra were analysed separately, O_3 treatment had a significant effect on leaf reflectance in every month of measurement (July, August, September $P < 0.001$, October $P = 0.014$).

Inclusion of the month of measurement showed a highly significant effect on the reflectance spectra of sapling leaves ($P < 0.001$). O_3 treatment and month of measurement had a significant interactive effect ($P < 0.001$). The interaction between species, O_3 treatment, and month was also significant ($P = 0.040$).

Principal component analysis (PCA) on the hyperspectral library of leaf reflectance spectra showed that the first four principal components explained 95.4% of the total variation in the dataset. The first principal component (PC1) accounted for 59.3% of the total variation, while the second (PC2), third (PC3), and fourth (PC4) components explained 23%, 9.1%, 4% of the variation, respectively. PC1 is loaded evenly across the entire wavelength range, suggesting it captures the overall shape of the leaf reflectance curve (Fig. 3). Component 2 relates highly to the red edge associated with chlorophyll content around 680 nm. The third component relates strongly to the green reflectance peak at 540 nm and the red edge.

A large amount of the variation explained by the first two principal components relates to differences between species, as indicated by the strong spatial clustering of species in supplementary material Figure A.9. When species were plotted separately against the second and third principle components (Fig. 3), clustering emerged for the highest and lowest ozone treatments. Separation of the highest and lowest ozone treatments by principle

components 2 and 3 was clearest in oak saplings.

3.2.2. PLS-DA

The PLS-DA models built for each species were able to discriminate accurately between saplings exposed to different O_3 treatments based on the hyperspectral reflectance spectra of leaves.

For beech leaves, 34 components were optimal for O_3 treatment classification, which was a significant dimensionality reduction from the original hyperspectral data (supplementary material, Figure A.12). The overall accuracy of O_3 treatment classification of this model was 0.872. Classification of beech leaves exposed to the highest treatment was most accurate (0.923). The prediction plot of the cross-validation dataset showed that most misclassifications were assigned to neighbouring O_3

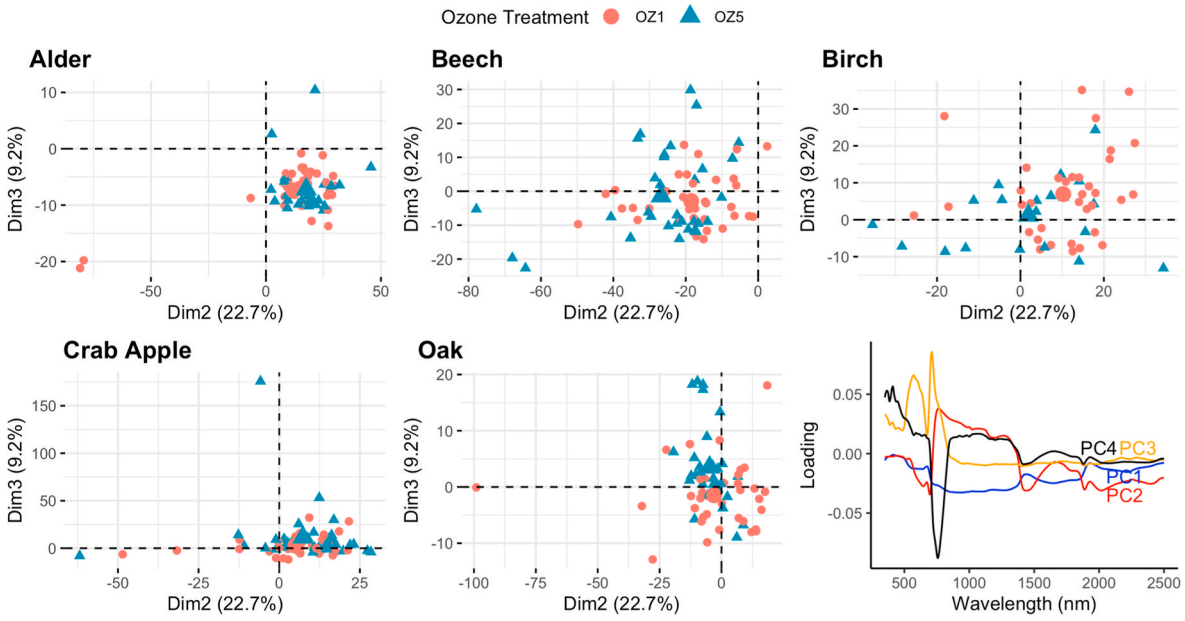

Fig. 3. Principal Component visualisation of the highest and lowest ozone treatments, split by species alongside the loading plot showing the wavelengths at which each of the first four principal components captures the most variation in the hyperspectral library of leaf reflectance.

treatments (e.g. leaves exposed to OZ4 misclassified as being exposed to OZ5 or OZ3). When only the highest and lowest O_3 treatments were used (OZ1 and 5), a PLS-DA model with only 16 components was 87.9% accurate at classifying leaf spectra to the correct O_3 treatment.

For oak saplings, a PLS-DA model comprised of 40 components produced an overall model accuracy of 0.859 (supplementary material, Figure A.15). The model's accuracy varied across the five O_3 treatments, with the highest accuracy seen for classifying leaves exposed to the

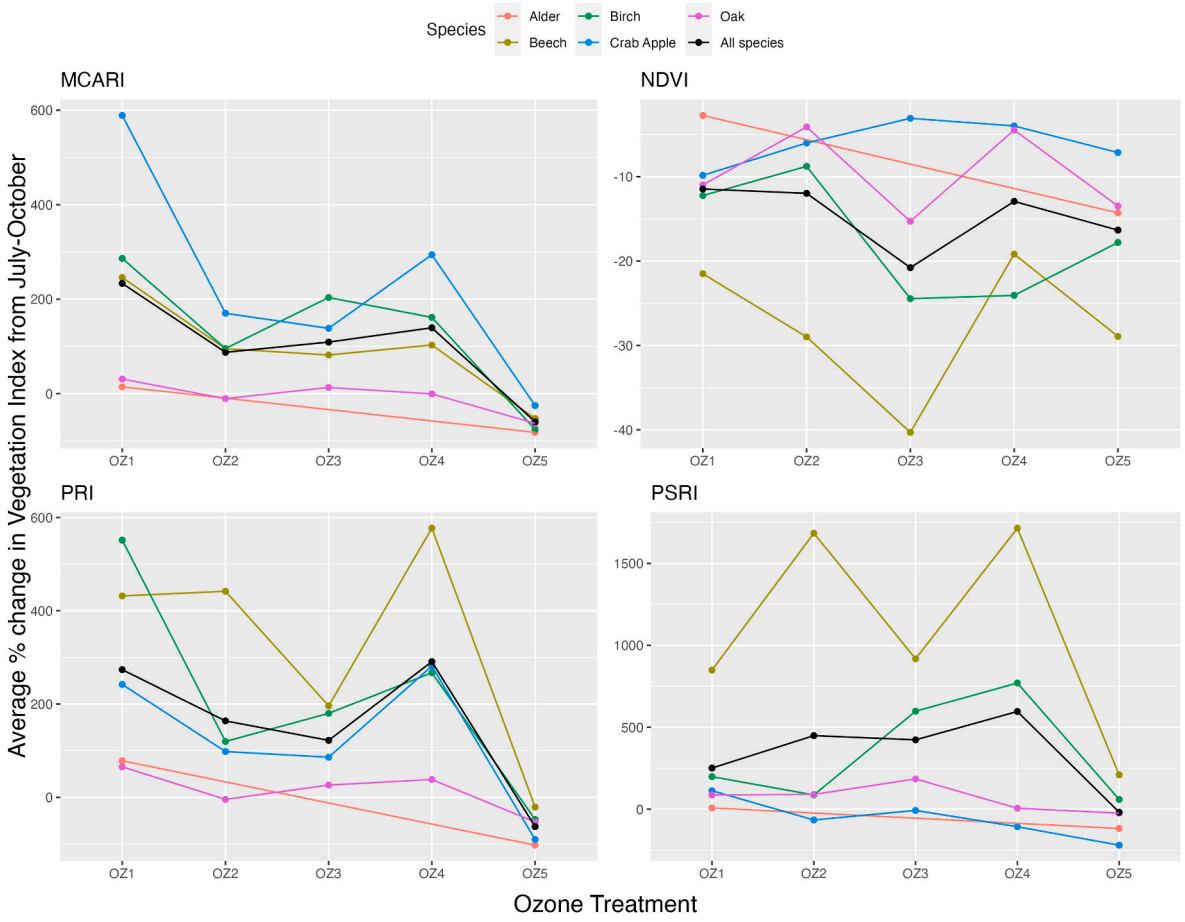

Fig. 4. Percentage change in vegetation indices from July–October across different O_3 treatments, coloured by species.

highest O_3 treatment OZ5 (0.902), and the lowest accuracy for OZ1 (0.797).

For alder saplings, a PLS-DA with 34 components, produced an overall accuracy of 0.913 (supplementary material, Figure A.12). For birch saplings, the optimal number of components for PLS-DA was 34, which produced an overall model accuracy of 0.898 (supplementary material, Figure A.13).

For crab apple the optimal number of components for PLS-DA was 37, which produced an overall model accuracy of 0.907 (supplementary material, Figure A.14).

These PLS-DA results show that O_3 exposure of leaves can be predicted from their hyperspectral reflectance. The calibration and validation datasets contained a random mix of spectra from different months, therefore classification of leaves to the correct O_3 treatment is not dependent on seasonality.

3.2.3. Vegetation indices

From the range of well-known vegetation indices calculated from leaf reflectance data, O_3 treatment only had a significant main effect on modified chlorophyll absorption in reflectance index (MCARI) (Fig. 4). Species and O_3 treatment had a significant interactive effect on all vegetation indices, as did the interaction of month and O_3 treatment. The MCARI results are explored in detail below. Photochemical reflectance index (PRI) and Plant senescence reflectance index (PSRI) results are also described as they were not suitable for PERMANOVA analysis. Full results for normalised difference vegetation index (NDVI) and red edge normalised difference vegetation index (RENDVI) can be found in the supplementary material.

Higher MCARI values correspond to a lower relative abundance of chlorophyll in the leaf. Broadly the MCARI of saplings increased during the growth season, as seen in Fig. 4, reflecting a seasonal decrease in chlorophyll. Although analysis of MCARI variance showed a significant main effect of ozone treatment, correlative analysis did not find a significant relationship between MCARI and ozone treatment ($\rho = -0.0239$, $P = 0.467$). This suggests although MCARI differed significantly between treatments, the relationship between ozone treatment and MCARI was not linear.

In terms of species-specific responses, we found that alder saplings showed limited changes in MCARI between O_3 treatments and over the growth season. The other four species showed the temporal dynamics described above and a clear difference in the MCARI of saplings in the highest O_3 treatment, as shown in Fig. 4.

Generally, the PRI of the saplings increased during the experimental period, except the saplings exposed to the highest O_3 treatment (Fig. 4, and supplementary material Figure A.17). The average PRI of saplings was not significantly affected by O_3 treatment alone in analysis of variance (KruskalWallis, $P > 0.05$), although a weak but significant positive correlation of PRI with ozone treatment was found ($\rho = 0.116$, $P < 0.001$).

Patterns in PSRI over time and with O_3 exposure vary by species, as visualised in supplementary material Figure A.18. PSRI of saplings in the highest O_3 treatment, OZ5, was significantly greater than those in all other treatments (Wilcoxon test, $P < 0.001$). However, the average PSRI of all species and months was not significantly affected by O_3 treatment overall (Kruskal-Wallis, $P > 0.05$). Correlative analysis revealed a weak but significant positive correlation of PSRI with ozone treatment as an ordinal variable ($\rho = 0.125$, $P < 0.001$).

Overall, the only vegetation index that showed significant differentiation between O_3 treatments and correlation with O_3 concentration across all species was MCARI. Other indices were able to distinguish between the highest and lowest O_3 treatments or differentiate O_3 treatments in some species. All vegetation indices were significantly affected by seasonal and interspecific variation.

3.2.4. Normalised difference spectral indices

To determine the best wavelengths to use for a normalised difference spectral index (NDSI) specific to O_3 stress, the strength of correlation between pairs of wavelengths and visual ozone damage were analysed as per equation (1) and plotted as a heatmap in Fig. 5.

When all species were combined, wavelengths in the 2200 nm–2300 nm SWIR region were identified as having the strongest Pearson Correlation to O_3 damage scores (Fig. 5). The combination of wavelengths with the highest correlation to O_3 damage was 2204 nm and 2248 nm, with a Pearson Correlation of 0.438.

These wavelengths were used to form a new reflective index specific to foliar O_3 damage:

$$\text{Ozone Damage Index (OzDI)} = \frac{A_{2204} - A_{2248}}{A_{2204} - A_{2248}} \quad (2)$$

where A_λ is the absorbance of wavelength λ.

OzDI ranged between 0.01 and 0.04, and increased over the growth season (Fig. 5, All Species). On average saplings exposed to ambient O_3 (OZ1) the OzDI of saplings was lowest in July, increased significantly by August and then remained stable until October. Saplings exposed to high O_3 (OZ5) showed a step-wise increase in OzDI each month. The highest OzDI values were seen in October in the highest O_3 treatment.

The highest OzDI values were seen in crab apple and beech saplings exposed to high O_3 (OZ4 and OZ5) in September and October. The lowest OzDI values were in Alder and Oak saplings in low O_3 treatments in July.

The average OzDI value was highest in the highest O_3 treatment in all species except oak, where OzDI was highest in the OZ4 treatment (Fig. 6, oak).

In this experiment, a cut off from OzDI >0.03 could be used to identify O_3 stressed saplings. Only saplings exposed to the highest two O_3 treatments had OzDI values > 0.03, although a seasonal and species-specific approach may be more precise.

OzDI performed well compared to existing vegetation indexes in differentiating O_3 treatments and when correlatively analysed. Spearman's rank correlation coefficient was calculated to determine the relationship between ozone treatment (as an ordinal variable) and OZDI value of leaves. The results indicate a significant positive relationship ($\rho = 0.180$, $P < 0.001$) with a stronger correlative coefficient than any of the other pre-existing vegetation indices tested (as detailed in 3.2.3).

In permutational analysis, variation in OzDI was more highly correlated to O_3 treatment, species and month than NDVI, RENDVI or MCARI in terms of *F*-Statistic (Table 2). There was also a highly significant interaction between the effects of species and O_3 treatment, species and month, O_3 treatment and month, and species, O_3 treatment and month ($F = 4.452$, $F = 5.16$, $F = 5.55$, $F = 1.71$ respectively, all $P < 0.001$).

The strength of correlation between pairs of wavelengths and visual ozone damage were also analysed for each species, and the performance of the species specific NDSI compared to OzDI.

In alder, the normalised difference of 1209 nm and 1218 nm was most strongly correlated to visual O_3 damage with a Pearson Correlation of 0.512. Spearman's rank correlation coefficient was calculated to determine the relationship between ozone treatment (as an ordinal variable) and the normalised difference of 1209 nm and 1218 nm for Alder saplings only. The results indicate a non-significant relationship ($\rho = 0.0058$, $P > 0.05$). When only alder saplings were analysed, OzDI had a positive relationship to ozone treatment ($\rho = 0.15$, $P = 0.0498$).

For birch saplings, the normalised difference between 674 nm and 680 nm correlated most strongly O_3 damage score, with a Pearson Correlation of 0.51. SWIR reflectance between 2200 nm and 2300 nm was also strongly correlated to visual O_3 damage in birch. Spearman's rank correlation analysis between this NDSI and ozone treatment of birch saplings did not show a relationship ($\rho = -0.00528$, $P > 0.05$). In birch saplings, OzDI showed a non-signficant positive relationship to ozone treatment ($\rho = 0.137$, $P > 0.05$).

O_3 damage score in crab apple saplings was most highly correlated to

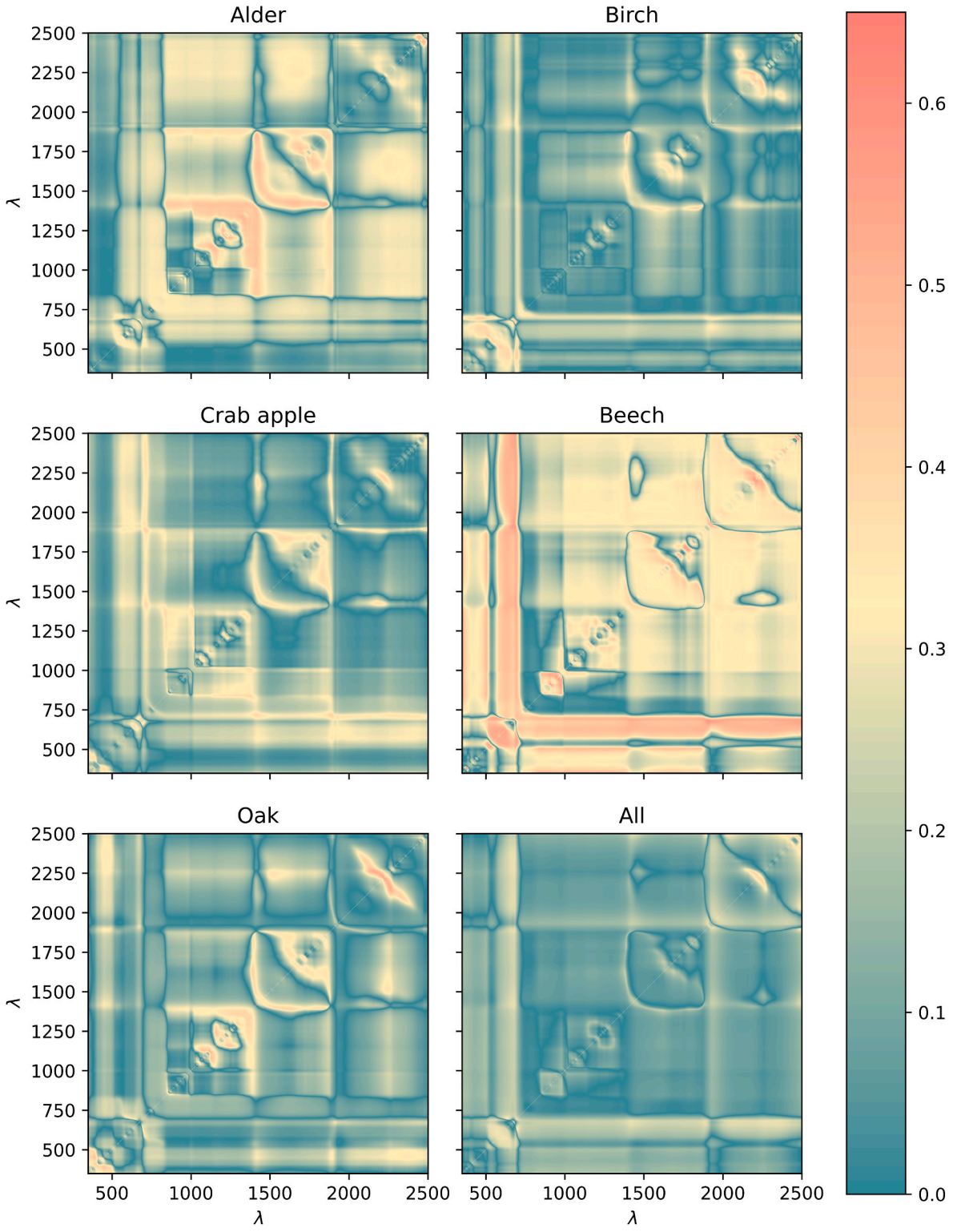

Fig. 5. Heat map of the Pearson's correlation coefficient between the normalised difference spectral index (NDSI) and visual O_3 damage score for all saplings, O_3 treatments and months of measurement.

the normalised difference of 2210 nm and 2228 nm, with a Pearson Correlation of 0.421. Spearman's rank correlation between ozone treatment and the normalised difference of 1209 nm and 1218 nm for crab apple saplings indicates a non-significant relationship ($\rho = 0.0742$, $P > 0.05$). When only crab appple saplings were analysed, OzDI had a strong positive relationship to ozone treatment ($\rho = 0.332$, $P < 0.001$).

For beech saplings the normalised difference of 956 nm and 958 nm was most strongly correlated to visual O_3 damage in beech, with a Pearson Correlation of 0.597. Spearman's rank correlation analysis between this NDSI and ozone treatment of beech saplings showed a significant negative relationship ($\rho = -0.175$, $P = 0.017$). In beech saplings, OzDI showed a highly signficant positive relationship to ozone treatment ($\rho = 0.291$, $P < 0.001$).

In oak, the normalised difference of 2221 nm and 2222 nm was most

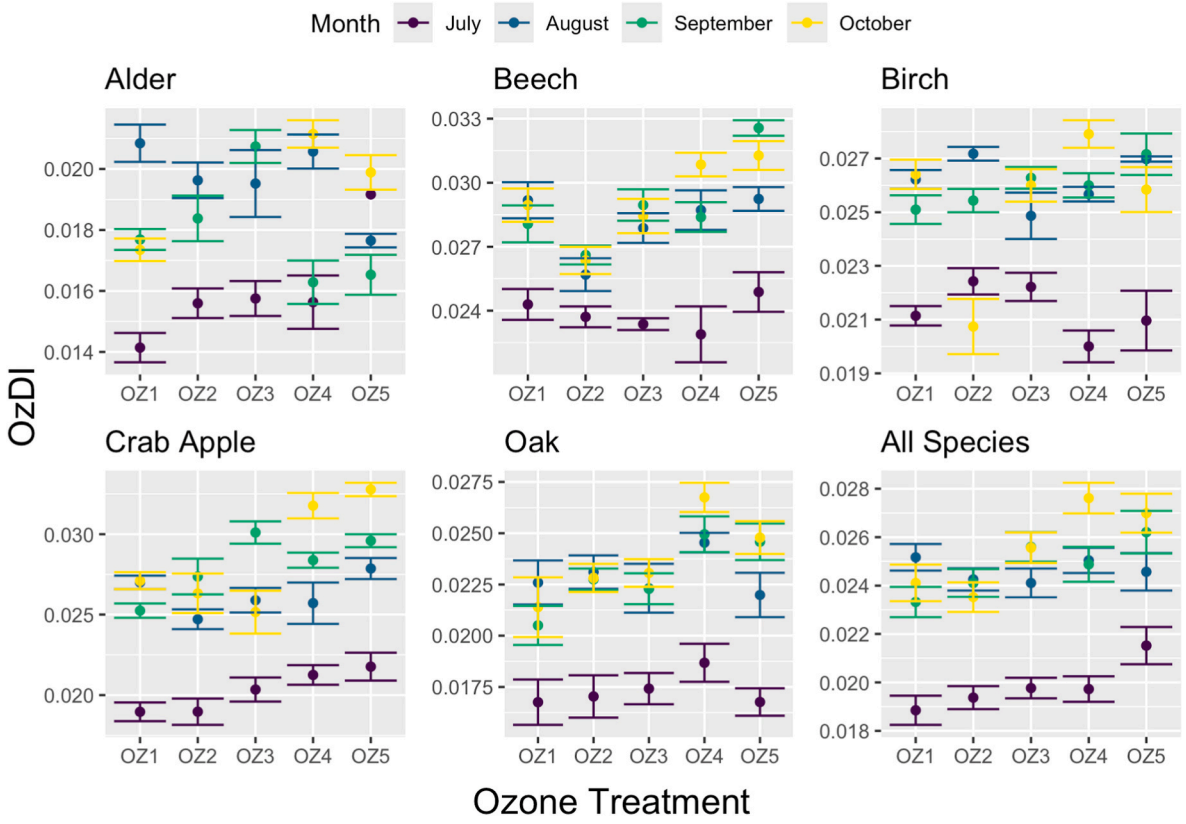

Fig. 6. OzDI vegetation index split by species in different ozone treatments, coloured by month of measurement.

Table 2
3-way permutational analysis of variance results for the impact of species, O_3 treatment and month of measurement on selected vegetation indices and the new OzDI index. 'd.o.f.' represents degrees of freedom. F represents the F statistic. Significance codes for P-values: ***: P < 0.001, **: P < 0.01, not stated: P > 0.05.999 permutations were used, and the Bray method was used to calculate pairwise distances from the spectral matrix.

Vegetation Index	NDVI			RENDVI			MCARI			OzDI		
	d.o.f.	F	P	d.o.f.	F	P	d.o.f.	F	P	d.o.f.	F	P
Species	4	24.06	0.001***	4	91.02	0.001***	4	70.92	0.001***	4	182.44	0.001***
O3 Treatment	4	1.94	0.075	4	1.97	0.069	4	3.79	0.002**	4	31.38	0.001***
Month	3	31.83	0.001***	3	47.84	0.001***	3	13.89	0.001***	3	182.12	0.001***
Species O3 Treatment	16	2.41	0.002**	16	4.99	0.001***	16	3.96	0.001***	16	4.45	0.001***
Species Month	12	5.03	0.001***	12	9.77	0.001***	12	10.66	0.001***			
O3 Treatment Month	12	1.4	0.13	12	2.89	0.001***	12	4.32	0.001***	12	5.55	0.001***
Species O3 Treatment Month	46	0.907	0.668	46	1.03	0.373.	46	1.49	0.003**	46	1.71	0.001***

strongly correlated to visual O_3 damage, with a Pearson Correlation of 0.577. These wavelengths characterise a similar part of the infrared spectrum as OzDI. Spearman's rank correlation analysis between this NDSI and ozone treatment of oak saplings showed a significant positive relationship ($\rho = 0.285$, $P < 0.001$). In oak saplings, OzDI also showed a highly signficant positive relationship to ozone treatment ($\rho = 0.301$, $P < 0.001$).

OzDI also outperformed the species specific normalised different indices calculated when tested across the entire spectral library. The alder specific NDSI (1209 nm and 1218 nm) did not correlate significantly with ozone treatment when analysed for all species. Neither did the birch NDSI of 674 nm and 680 nm. The crab apple NDSI (2210 nm and 2228 nm) was significantly positively correlated with ozone treatment across all species, but less strongly than OzDI ($\rho = 0.115$, $P < 0.001$). Similarly, the beech NDSI (956 nm and 958 nm) was significantly negatively correlated with ozone treatment across all species, but less strongly than OzDI ($\rho = -0.110$, $P < 0.001$). The oak NDSI (2221 nm and 2222 nm) was also significantly correlated with ozone treatment across all species, but again less strongly than OzDI ($\rho = -0.113$, $P < 0.001$).

4. Discussion

All species exhibited characteristic foliar O_3 damage when exposed to high O_3 treatments, consistent with previous studies that have reported a positive relationship between O_3 exposure and visual leaf injury (Clark et al., 2000; Gosselin et al., 2020). Although the growth of saplings during initial treatment was not affected by O_3, high O_3 reduced growth in the saplings measured one year after initial exposure. Carry-over effects on sapling growth following O_3 stress were also found in several other studies (Oksanen and Saleem, 1999; Riikonen et al., 2008).

The combination of visible foliar damage and reduced growth in the following season indicates that the saplings experienced O_3 damage proportional to O_3 exposure.

The hyperspectral leaf reflectance of saplings exposed to different O_3 concentrations showed clear differentiation despite the large seasonal and interspecific variation. A sharp reflectance peak at 750 nm was

visible in all leaves in the highest O_3 treatment in July. Chlorophyll fluoresces at 750 nm (Pablo et al., 2000), it is likely this peak is caused by fluorescence influencing the reflectance spectrum. Models based on the principle components of the hyperspectral dataset were able to accurately predict the O_3 treatment which new leaf spectra had been exposed to. The changes in reflectance of the visible region in saplings exposed to high O_3 corroborate the visible injury observed. Leaf reflectance spectra indicate changes in the carbohydrate content within the leaf associated with the cellulose reflectance peak, which may be related to the carryover effects of O_3 on the growth of the saplings observed. Therefore, changes in hyperspectral reflectance support the physical measurements that detected O_3 damage.

Hyperspectral data is rapid to collect and the leafclip attachment with active light source produces a high signal to noise ratio. The number of repeats of physiological and physical measurements taken was limited by their time-consuming nature, whereas over 1450 spectra were taken capturing variation between leaves, saplings, and treatments. The high number of spectra measured allowed the effect of O_3 to be identified amongst other strong sources of variation such as species and seasonality. Outside of a controlled experimental environment, the repeatability and high-throughput advantages of spectral data would be even more pronounced.

Changes in hyperspectral reflectance of saplings exposed to high O_3 also revealed additional responses not identified by other measurements. For example, high O_3 reduced NIR reflectance which is associated with the cellular structure and spongy mesophyll of the leaf. Previous studies have found cellular structure to be modified under high O_3 exposure in broadleaf species (Oksanen et al., 2005).

NDSI analysis showed species specific differences in the wavelengths most strongly correlated to visible ozone damage, however none of these outperformed OzDI in terms of correlation to ozone treatment across all species. The species specific NDSI for crab apple and oak characterised a very similar part of the SWIR region as OzDI. For leaf reflectance measurements taken with a lower resolution spectrometer, OzDI could be rounded to 2200 nm and 2250 nm to characterise this key peak.

Our NDSI analysis revealed a stronger correlation between visible O_3 injury and the SWIR region of leaf reflectance than regions associated with pigments. Reflectance in the SWIR region is associated with leaf cellulose, starch, and sugar content, as well as water content (Curran, 1989; Cheng et al., 2011). Studies have found O_3 stress reduces the hemicellulose content of leaves (Oksanen et al., 2005).

The variation in OzDI between O_3 treatments may therefore be accompanied by changes in the cellulose, starch, and sugar content in O_3 stressed leaves, as well as the reduced water content due to stomatal closure.

Hyperspectral reflectance also revealed the complexity of O_3 responses which are not always linear. In several regions of the spectra, such as the green reflectance peak and NIR, the saplings in intermediate O_3 treatments had the highest reflectance. Hormesis describes the stimulatory effect of low doses of pollutants or toxins on plants and animals. A hormetic response to O_3 has been identified in many studies, as summarised by Agathaokleous et al. (Agathokleous et al., 2019). Chlorophyll concentration is known to show hormetic dynamics in response to low doses of toxins including O_3 (Agathokleous et al., 2020). Understanding the complexities of dosage-dependent O_3 responses is vital to assess O_3 damage in natural settings, and hyperspectral reflectance provided higher resolution insight into the dose response of foliar O_3 damage.

Vegetation indices calculated from the hyperspectral reflectance were able to show changes in the response to O_3 stress over time. The high PRI and MCARI of saplings in the highest O_3 treatment during the first month of O_3 treatment suggests an initial acute O_3 response which was not maintained over chronic exposure, potentially showing acclimation to high O_3 stress. NDVI characterises the red edge like MCARI but does not include the green peak, and did not show this trend. This indicated the initial increase in MCARI and PRI in response to high O_3 was underpinned by changes in the green peak reflectance. A fall in green peak reflectance can either be caused by a drop in chlorophyll or carotenoids or an increase in anthocyanin concentration. Anthocyanins are an antioxidant known to be upregulated in response to the oxidative stress caused by high O_3 exposure (Chalker-Scott, 1999).

Although our study used saplings, there is evidence to suggest similar O_3 damage is found between young and mature trees. Visible O_3 injury to beech saplings in phytotrons was found at similar AOT40 levels to mature trees at a free air manipulation experiment (Baumgarten et al., 2000). Other research has shown inconsistent scaling of leaf-level responses to O_3 between juvenile and mature trees, dependent on compensation mechanisms and stomatal responses (Kolb and Matyssek, 2003; Kolb et al., 1997). Considering this, although our results indicate hyperspectral detection of O_3 damage is a viable method in broadleaf species, application of this method to mature trees and outside controlled conditions would require further testing. For reforestation however, hyperspectral detection of O_3 damage to young saplings is highly relevant and could be deployed to help understand variable success rates in planting initiatives.

The controlled conditions of the solardomes allow characterisation of O_3 damage using a lower number of replicates than would be needed in the field, due to reduced microclimate variability. However, in forests O_3 deposition varies along vertical profiles and temporally due to canopy fluxes (Finco et al., 2018). Any field trial of hyperspectral detection of O_3 damage would need to capture this microclimatic variability particularly for saplings in the understorey.

Hyperspectral data generally is much more scalable than traditional methods of O_3 damage detection. Hyperspectral instruments can be mounted on UAVs or aircraft. Vegetation indices can be translated across spectroscopy instruments of varying resolution to including multispectral sensors. Leaf scale detection of O_3 damage may be upscaled to canopy level detection, although this would require further study to ascertain the strength of the O_3 damage signal when remotely sensing reflectance.

Leaf reflectance was significantly affected by O_3 treatment at all measurement points throughout the growth season, although in by the end of the season this effect was weaker. O_3 is known to have a cumulative damaging effect on vegetation (Per Erik Karlsson, 2009), however, seasonality has a large influence on the reflectance of deciduous trees due to changes in pigments and water content as senescense approaches. In all analyses the effect of species and month of measurement was greater than the effect of O_3 treatment, emphasising the importance of taking into account these variables when assessing O_3 damage. For example, a higher than average OzDI would need to be interpreted in context of the species and when in the growth season the measurement was taken, as is the case for most vegetation indices used to measure plant stress.

Changes in the reflectance signal of O_3 damaged leaves were broadly shared by all the broadleaf species tested, despite some species-specific differences. This suggests that canopy level analysis of O_3 damage could be feasible using a mixed species model, although this approach would need to be further tested in adult trees. Canopy level assessment of O_3 damage via hyperspectral reflectance would allow rapid evaluation of the impacts of tropospheric O_3 on forests, only currently possible by labour-intensive or destructive methods. To reliably attribute foliar damage to O_3, other abiotic and biotic stressors would need to be excluded. The changes to reflectance in the visible region and some vegetation indices (such as MCARI) observed are common to many stress responses. However, the multivariate changes observed throughout the fully hyperspectral range are more likely to be unique to ozone stress. Trialling hyperspectral detection of foliar O_3 damage in adult trees alongside high resolution O_3 measurements would be a prudent next step in the development of remote sensing O_3 damage to forests.

4.1. Conclusions

Our results demonstrate that hyperspectral reflectance can be used to identify O_3 damage in broadleaf saplings and differentiate between plants exposed to different concentrations of O_3 exposure. Hyperspectral leaf reflectance was able to distinguish saplings exposed to different O_3 treatments despite high inter and intra-specific variation. The entire hyperspectral reflectance profile of O_3 damaged leaves indicates a multivariate signal of O_3 damage, comprised of changes in pigments, leaf structure and water content. Wavelengths in the SWIR used to develop the new OzDI index could be used in conjunction with MCARI to predict the O_3 exposure of broadleaf trees in a seasonal and species-based context. This work represents a critical first step in developing a remote sensing assessment for O_3 damage to forests, which now needs to be tested in adult trees and non-experimental settings.

CRediT authorship contribution statement

Anna Lee Jones: Writing – review & editing, Writing – original draft, Visualization, Validation, Software, Resources, Project administration, Methodology, Investigation, Formal analysis, Data curation, Conceptualization. **Adam Ormondroyd:** Writing – review & editing, Software, Formal analysis. **Felicity Hayes:** Writing – review & editing, Supervision, Methodology. **Elizabeth S. Jeffers:** Writing – review & editing, Supervision, Conceptualization.

Declaration of competing interest

The authors declare that they have no known competing financial interests or personal relationships that could have appeared to influence the work reported in this paper.

Data availability

Data will be made available on request.

Acknowledgements

This work was supported by the Natural Environment Research Council [grant number NE/S007474/1]. The SVC HR-1024i, leaf clip-reflectance probe attachment, and reflectance panels, were loaned from the National Environment Research Council Field Spectroscopy Facility (NERC FSF) under FSF internal loan number 884.1121. The authors gratefully acknowledge NERC FSF for this loan, and for the training and technical advice provided.

Appendix A. Supplementary data

Supplementary data to this article can be found online at https://doi.org/10.1016/j.envpol.2024.124642.

References

Agathokleous, Evgenios, Araminiene, Valda, Belz, Regina G., 2019. Vicent calatayud, Alessandra de Marco, marisa domingos, ZhaoZhong feng, yasutomo hoshika, mitsutoshi kitao, takayoshi koike, elena paoletti, costas J. Saitanis, pierre sicard, and edward J. Calabrese. A quantitative assessment of hormetic responses of plants to ozone. Environ. Res. 176, 108527.

Agathokleous, Evgenios, Feng, ZhaoZhong, Peñuelas, Josep, 2020. Chlorophyll hormesis: are chlorophylls major components of stress biology in higher plants? Sci. Total Environ. 726, 138637.

Ainsworth, Elizabeth, Yendrek, Craig, Sitch, Stephen, Collins, William, Emberson, Lisa, 2012. The effects of tropospheric ozone on net primary productivity and implications for climate change *. Annu. Rev. Plant Biol. 63, 637–661.

Amanda, J., Holder, Hayes, Felicity, 2022. Substantial yield reduction in sweet potato due to tropospheric ozone, the dose-response function. Environ. Pollut. 304, 119209.

M. R. Ashmore. Assessing the future global impacts of ozone on vegetation. Plant Cell Environ., 28(8):949–964,2005. eprint: https://onlinelibrary.wiley.com/doi/pdf/10.1111/j.13653040.2005.01341.x.

Baumgarten, M., Werner, H., Häberle, K.H., Emberson, L.D., Fabian, P., Matyssek, R., 2000. Seasonal ozone response of mature beech trees (*Fagus sylvatica*) at high altitude in the Bavarian forest (Germany) in comparison with young beech grown in the field and in phytotrons. Environ. Pollut. 109 (3), 431–442.

Claudia Beleites and Valter Sergo. hyperSpec: a Package to Handle Hyperspectral Data Sets in R, 100.

Brace, Sarah, Peterson, David L., Bowers, Darci, 1999. A Guide to Ozone Injury in Vascular Plants of the Pacific Northwest. Technical Report PNW-GTR-446, U.S. Department of Agriculture, Forest Service. Pacific Northwest Research Station, Portland, OR.

Brewster, Clare, Fenner, Nathalie, Hayes, Felicity, 2024. Chronic Ozone Exposure Affects Nitrogen Remobilization in Wheat at Key Growth Stages. Science of the Total Environment, p. 168288, 908.

Calzone, Antonella, Cotrozzi, Lorenzo, Remorini, Damiano, Lorenzini, Giacomo, Nali, Cristina, Pellegrini, Elisa, 2021. Oxidative stress assessment by a spectroscopic approach in pomegranate plants under a gradi- ent of ozone concentrations. Environ. Exp. Bot. 182, 104309.

Chalker-Scott, Linda, 1999. Environmental significance of anthocyanins in plant stress responses. Photochem. Photobiol. 70 (1), 1–9 eprint. https://onlinelibrary.wiley.com/doi/pdf/10.1111/j.17511097.1999.tb01944.x.

Charles, R., Harris, Jarrod Millman, K., J van der Walt, St′efan, Gommers, Ralf, Virtanen, Pauli, Cournapeau, David, Wieser, Eric, Taylor, Julian, Sebastian, Berg, Nathaniel J, Smith, Robert, Kern, Matti, Picus, Stephan, Hoyer, van Kerkwijk, Marten H., Matthew, Brett, Haldane, Allan, Fern′andez del R′ıo, Jaime, Mark Wiebe, Peterson, Pearu, G′erard-Marchant, Pierre, Sheppard, Kevin, Reddy, Tyler, Weckesser, Warren, Abbasi, Hameer, Gohlke, Christoph, Oliphant, Travis E., 2020. Array programming with NumPy. Nature 585, 357–362.

Cheng, T., Rivard, B., Sa′nchez-Azofeifa, A., 2011. Spectroscopic determination of leaf water content using continuous wavelet analysis. Rem. Sens. Environ. 115 (2), 659–670.

Clark, A.J., Landolt, W., Bucher, J.B., Strasser, R.J., 2000. Beech (Fagus sylvatica) response to ozone exposure assessed with a chlorophyll a fluorescence performance index. Environ. Pollut. 109 (3), 501–507.

Curran, Paul J., 1989. Remote sensing of foliar chemistry. Rem. Sens. Environ. 30 (3), 271–278.

Diem, Jeremy E., 2002. Remote assessment of forest health in Southern Arizona, USA: evidence for ozone-induced foliar injury. Environ. Manag. 29 (3), 373–384.

Feng, Zhaozhong, 2018. Patrick Büker, H°Akan Pleijel, Lisa Emberson, Per Erik Karlsson, and Johan Uddling. A unifying explanation for variation in ozone sensitivity among woody plants. Global Change Biol. 24 (1), 78–84. https://onlinelibrary.wiley.com/doi/pdf/10.1111/gcb.13824.

Finco, Angelo, Coyle, Mhairi, Nemitz, Eiko, Marzuoli, Riccardo, Chiesa, Maria, Loubet, Benjamin, Fares, Silvano, Diaz-Pines, Eugenio, Gasche, Rainer, Gerosa, Giacomo, 2018. Characterization of Ozone Deposition to a Mixed Oak–Hornbeam Forest – Flux Measurements at Five Levels above and inside the Canopy and Their Interactions with Nitric Oxide. Atmospheric Chemistry and Physics. Publisher, Copernicus GmbH, pp. 17945–17961, 18(24).

Francini, A., Nali, C., Picchi, V., Lorenzini, G., 2007. Metabolic changes in white clover clones exposed to ozone. Environ. Exp. Bot. 60 (1), 11–19.

Gaudel, A., Cooper, O.R., Ancellet, G., Barret, B., Boynard, A., P Burrows, J., Clerbaux, C., Coheur, P.-F., Cuesta, J., Cuevas, E., Doniki, S., Dufour, G., Ebojie, F., Foret, G., Garcia, O., Granados-Muñoz, M.J., Hannigan, J.W., Hase, F., Hassler, B., Huang, G., Hurtmans, D., Jaffe, D., Jones, N., Kalabokas, P., Kerridge, B., Kulawik, S., Latter, B., Leblanc, T., Le Flochmöen, E., Lin, W., Liu, J., Liu, X., Mahieu, E., McClure-Begley, A., Neu, J.L., Osman, M., Palm, M., Petetin, H., Petropavlovskikh, I., Querel, R., Rahpoe, N., Rozanov, A., Schultz, M.G., Schwab, J., Siddans, R., Smale, D., Steinbacher, M., Tanimoto, H., Tarasick, D.W., Thouret, V., Thompson, A.M., Trickl, T., Weatherhead, E., Wespes, C., Worden, H.M., Vigouroux, C., Xu, X., Zeng, G., Ziemke, J., 2018. Tropospheric Ozone Assessment Report: present-day distribution and trends of tropospheric ozone relevant to climate and global atmospheric chemistry model evaluation. Elementa: Science of the Anthropocene 6, 39.

Gosselin, Nichole, Sagan, Vasit, Maimaitiyiming, Matthew, Fishman, Jack, Belina, Kelley, Podleski, Ann, Maimaitijiang, Maitiniyazi, Anbreen Bashir, Jayashree Balakrishna, Dixon, Austin, 2020. Using Visual Ozone Damage Scores and Spectroscopy to Quantify Soybean Responses to Background Ozone. Remote Sensing. Number: 1 Publisher, Multidisciplinary Digital Publishing Institute, p. 93, 12(1.

Gottardini, Elena, Calatayud, Vicent, Ferretti, Marco, Haeni, Matthias, Schaub, Marcus, 2016. Spatial and temporal distribution of ozone symptoms across Europe from 2002 to 2014. BFW-Dokumentation 23, 73–82.

Gab, Martina, Hoffmann, Katharina, Lobe, Melanie, Metzger, Rut, Ooyen, Sven van, Elbers, Gereon, Köllner, Barbara, 2006. NIR-spectroscopic investigation of foliage of ozone-stressed Fagus sylvatica trees. J. For. Res. 11 (2), 69–75. https://doi.org/10.1007/s10310-005-0186-3. Publisher: Taylor & Francis eprint.

Hattie, R., Roberts, Ian, C., Dodd, Hayes, Felicity, Ashworth, Kirsti, 2022. Chronic tropospheric ozone exposure reduces seed yield and quality in spring and winter oilseed rape. Agric. For. Meteorol. 316, 108859.

Hayes, Felicity, Williamson, Jennifer, Mills, Gina, 2015. Species-specific responses to ozone and drought in six deciduous trees. Water, Air, Soil Pollut. 226 (5), 156.

Hunter, John D., 2007. Matplotlib: a 2D graphics environment. Comput. Sci. Eng. 9 (3), 90–95. Publisher: IEEE.

Intergovernmental Panel on Climate Change (IPCC), 2023. Climate Change 2021 – The Physical Science Basis: Working Group I Contribution to the Sixth Assessment Report of the Intergovernmental Panel on Climate Change. Cambridge University Press.

Kangasjarvi, J., Talvinen, J., Utriainen, M., Karjalainen, R., 1994. Plant defence systems induced by ozone. Plant Cell Environ. 17 (7), 783–794. https://onlinelibrary.wiley.com/doi/pdf/10.1111/j.13653040.1994.tb00173.x.

Kefauver, Shawn C., 2013. Using Topographic and Remotely Sensed Variables to Assess Ozone Injury to Conifers in the Sierra Nevada (USA) and Catalonia (Spain). Remote Sensing of Environment, p. 11.

Kolb, T.E., Matyssek, R., 2003. Limitations and perspectives about scaling ozone impacts in trees. In: Developments in Environmental Science. Elsevier, pp. 141–173.

Kolb, T.E., Fredericksen, T.S., Steiner, K.C., Skelly, J.M., 1997. Issues in scaling tree size and age responses to ozone: a review. Environ. Pollut. 98 (2), 195–208.

Kucheryavskiy, Sergey, 2020. Mdatools – R package for chemometrics. Chemometr. Intell. Lab. Syst. 198, 103937.

Young Lee. SpecDAL 2.0.0.

Levy, H., 1971. Normal atmosphere: large radical and formaldehyde concentrations predicted. Science. American Association for the Advancement of Science Section: Reports 173 (3992), 141–143. Publisher.

Marchica, Lor′e, Cotrozzi, Lorenzini, 2019. Nali, pellegrini, and remorini. Early detection of sage (salvia officinalis L.) responses to ozone using reflectance spectroscopy. Plants 8 (9), 346.

Meroni, Michele, Rossini, Micol, Picchi, Valentina, Panigada, Cinzia, Cogliati, Sergio, Nali, Cristina, Colombo, Roberto, 2008a. Assessing steadystate fluorescence and PRI from hyperspectral proximal sensing as early indicators of plant stress: the case of ozone exposure. Sensors. Molecular Diversity Preservation International 8 (3), 1740–1754. Number: 3 Publisher.

Meroni, M., Picchi, V., Rossini, M., Cogliati, S., Panigada, C., Nali, C., Lorenzini, G., Colombo, R., 2008b. Leaf level early assessment of ozone injuries by passive fluorescence and photochemical reflectance index. Int. J. Rem. Sens. 29 (17–18), 5409–5422.

Mickley, L.J., Murti, P.P., Jacob, D.J., Logan, J.A., Koch, D.M., Rind, D., 1999. Radiative forcing from tropospheric ozone calculated with a unified chemistry-climate model. J. Geophys. Res. Atmos. 104 (D23), 30153–30172. https://agupubs.onlinelibrary.wiley.com/doi/pdf/10.1029/1999JD900439.

Mills, Gina, Hayes, Felicity, Simpson, David, Emberson, Lisa, Norris, David, Harmens, Harry, Büker, Patrick, 2011. Evidence of widespread effects of ozone on crops and (semi-)natural vegetation in Europe (1990–2006) in relation to AOT40- and flux-based risk maps. Global Change Biol. 17 (1), 592–613. https://onlinelibrary.wiley.com/doi/pdf/10.1111/j.13652486.2010.02217.x.

Moon, S., Kim, Charles, L., Mulchi, Craig, S., Daughtry, T., McMurtrey, James E., 2004. Assessment of combined effects of elevated tropospheric O3 and CO2 on soybean under well-watered and restricted soil moisture conditions by multispectral fluorescence imaging techniques. In digital imaging and spectral techniques: applications to precision agriculture and crop physiology. John Wiley & Sons, Ltd pages 223–253. https://onlinelibrary.wiley.com/doi/pdf/10.2134/asaspecpub66.c17.

Nuvolone, Daniela, Petri, Davide, Voller, Fabio, 2018. The effects of ozone on human health. Environ. Sci. Pollut. Control Ser. 25 (9), 8074–8088.

Oksanen, E., Saleem, A., 1999. Ozone exposure results in various carry-over effects and prolonged reduction in biomass in birch (Betula pendula Roth). Plant Cell Environ. 22 (11), 1401–1411. https://onlinelibrary.wiley.com/doi/pdf/10.1046/j.1365-3040.1999.00501.x.

Oksanen, Elina, Riikonen, Johanna, Kaakinen, Seija, Holopainen, Toini, Vapaavuori, Elina, 2005. Structural characteristics and chemical composition of birch (Betula pendula) leaves are modified by increasing CO2 and ozone. Global Change Biol. 11 (5), 732–748. https://onlinelibrary.wiley.com/doi/pdf/10.1111/j.13652486.2005.00938.x.

Oksanen, Jari, Kindt, Roeland, Pierre Legendre, Bob O'Hara, Simpson, Gavin L., Solymos, Peter, Henry, M., Stevens, H., Wagner, Helene, 2008. Vegan: Community Ecology Package.

Pablo, J., Zarco-Tejada, John, R., Miller, Gina, H., Mohammed, Noland, Thomas L., 2000. Chlorophyll fluorescence effects on vegetation apparent reflectance: I. Leaf-level measurements and model simulation. Rem. Sens. Environ. 74 (3), 582–595.

Per Erik Karlsson, 2009. H°Akan Pleijel, Helena Danielsson, Gunilla Pihl Karlsson, Kristin Piikki, and Johan Uddling. Evidence for impacts of nearambient ozone concentrations on vegetation in Southern Sweden. AMBIO A J. Hum. Environ. 38 (8), 425–432.

Proietti, C., Anav, A., De Marco, A., Sicard, P., Vitale, M., 2016. A multisites analysis on the ozone effects on Gross Primary Production of European forests. Sci. Total Environ. 556, 1–11.

Riikonen, Johanna, Kets, Karte, Darbah, Joseph, Oksanen, Elina, Sober, Anu, Vapaavuori, Elina, Kubiske, Mark E., Nelson, Neil, David, F., 2008. Karnosky. Carbon gain and bud physiology in Populus tremuloides and Betula papyrifera grown under long-term exposure to elevated concentrations of CO2 and O3. Tree Physiol. 28 (2), 243–254.

Saxe, H., 2002. Physiological Responses of Trees to Ozone - Interactions and Mechanisms. Current Topics in Plant Biology, Volume 3. Publisher, Research Trends, pp. 27–55.

Schaub, M., Calatayud, V., Ferretti, M., G Lövblad, G Brunialti, Krause, G., Sanz, M.J., 2016. Part VIII: monitoring of ozone injury. In: ICP Forests Programme Co-ordinating Centre, U.N.E.C.E. (Ed.), Manual on Methods and Criteria for Harmonized Sampling, Assessment, Monitoring and Analysis of the Effects of Air Pollution on Forests. Technical Report, Thünen Institute of Forest Ecosystems.

Sicard, P., Vas, N., Calatayud, V., Garcia-Breijo, F.J., Reig-Armiñana, J., Sanz, M.J., Dalstein-Richier, L., 2010. Dommages forestiers et pollution a′ l'ozone dans les r′eserves naturelles : le cas de l'arolle dans le sud-est de la France -. *For*ˆ*et M′editerran′eenne*. XXXI(3) 273.

Treshow, Michael, 1970. Ozone damage to plants. Environ. Pollut. 1 (2), 155–161. October 1970.

Van Rossum, Guido, Drake, Fred L., 2009. Python 3 Reference Manual. CreateSpace, Scotts Valley, CA.

Victoria, E., Wittig, Elizabeth, A., Ainsworth, Long, Stephen P., 2007. To what extent do current and projected increases in surface ozone affect photosynthesis and stomatal conductance of trees? A meta-analytic review of the last 3 decades of experiments. Plant Cell Environ. 30 (9), 1150–1162. https://onlinelibrary.wiley.com/doi/pdf/10.1111/j.13653040.2007.01717.x.

Vingarzan, Roxanne, 2004. A review of surface ozone background levels and trends. Atmos. Environ. 38 (21), 3431–3442.